SANDIA REPORT
SAND2021-12108
Printed September 2021

Sandia National Laboratories

City-Wide Distributed Roof-Top Photovoltaic System Adoption Forecast, Grid Impact Simulation, & Neighborhood Microgrid Contribution Assessment

C. Birk Jones, William F. Vining, Thad Haines

Prepared by
Sandia National Laboratories
Albuquerque, New Mexico 87185
Livermore, California 94550

Issued by Sandia National Laboratories, operated for the United States Department of Energy by National Technology & Engineering Solutions of Sandia, LLC.

Available to DOE and DOE contractors from

U.S. Department of Energy
Office of Scientific and Technical Information
P.O. Box 62
Oak Ridge, TN 37831

Telephone: (865) 576-8401
Facsimile: (865) 576-5728
E-Mail: reports@osti.gov
Online ordering: http://www.osti.gov/scitech

Available to the public from

U.S. Department of Commerce
National Technical Information Service
5301 Shawnee Road
Alexandria, VA 22312

Telephone: (800) 553-6847
Facsimile: (703) 605-6900
E-Mail: orders@ntis.gov
Online order: https://classic.ntis.gov/help/order-methods

City-Wide Distributed Roof-Top Photovoltaic System Adoption Forecast, Grid Impact Simulation, & Neighborhood Microgrid Contribution Assessment

C. Birk Jones
Sandia National Laboratories
P.O. Box 5800
Albuquerque, NM 87185-9999
cbjones@sandia.gov

William F. Vining
Sandia National Laboratories
P.O. Box 5800
Albuquerque, NM 87185-9999
wfvinin@sandia.gov

Thad Haines
Sandia National Laboratories
P.O. Box 5800
Albuquerque, NM 87185-9999
jthaine@sandia.gov

SAND2021-12108

ABSTRACT

The adoption of distributed photovoltaic (PV) systems grew significantly in recent years. Market projections anticipate future growth for both residential and commercial installations. To understand grid impacts associated with distributed PV, useful hosting capacity studies require accurate representations of the spatial distribution of PV adoptions. Prediction of PV locations and numbers depends on median income data, building use zoning maps, and permit records to understand existing trends and predict future adoption rates and locations throughout an entire city. Using the PV adoption data, advanced and realistic simulations were performed to capture the distributed PV impacts on the grid. Also, using graph theory community detection hundreds of neighborhood microgrids can be discovered for the entire city by identifying densely connected loads that are sparsely connected to other communities. Then, based on the PV adoption predictions, this work identified the contribution of PV within each of the newly discovered graph theory defined microgrid communities.

ACKNOWLEDGMENT

Thanks to Sandia National Laboratories LDRD Resilient Energy System program for funding this work.

CONTENTS

LIST OF FIGURES

LIST OF TABLES

SUMMARY

This paper describes the creation and implementation of a city-wide forecast methodology, grid simulation, and PV for microgrid analysis that defines the impact of distributed photovoltaic (PV) systems. First, a PV adoption forecast methodology predicts future locations based on census median income, building use zoning, and historical permit data. The foredcast predicts PV adoptions 5, 10, 20, and 30 years into the future. Figure 0-1 depicts the spatial density of the distribution PV locations in the past, today, and in the future for Santa Fe, New Mexico.

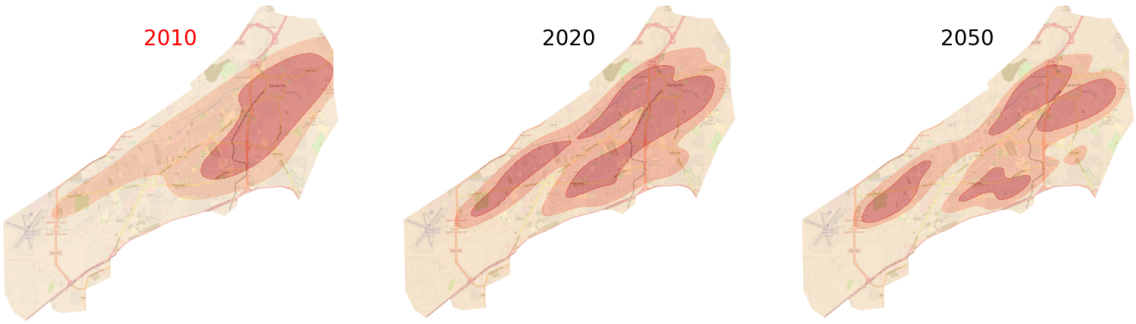

(a) PV Location Density 2010 **(b) PV Location Density 2020** **(c) PV Location Density 2050**

Figure 0-1 Plots (a) and (b) show the historical progression of the PV system installations starting in 2010 and then in 2020. Then, (c) describes the predicted location of PV systems in 2030.

Then, using the HELICS co-simulation environment and a graph theory community detection algorithm, this work implements a methodology that discovers potential neighborhood microgrid locations and estimates the contribution of roof-top PV for a single day of operations. Figure 0-2 shows the microgrid locations using dots scattered throughout the city of Santa Fe and depicts the PV contribution as a percentage of the load for a single day using the dot sizes and colors.

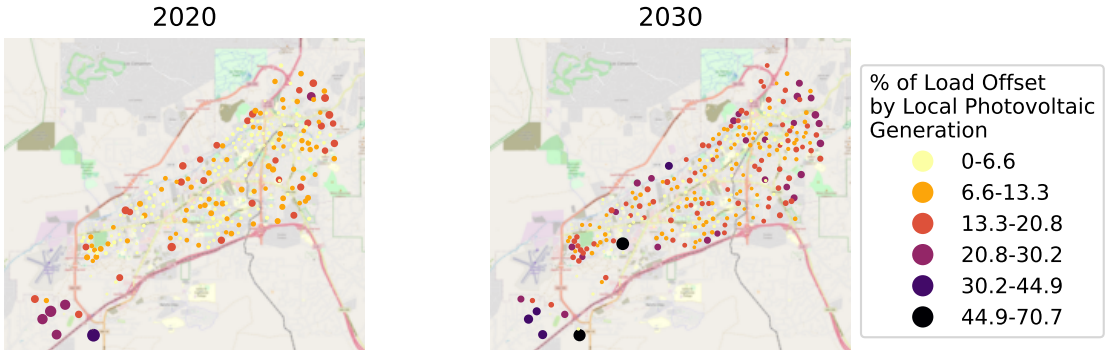

Figure 0-2 These images show the graph theory defined microgrid communities and the percentage of load offset by distributed PV in 2020 and 2030 for a single day of operations.

NOMENCLATURE

DER Distributed Energy Resource

DG Distributed Generation

EV Electric Vehicles

EPS Electric Power System

HVAC Heating, Ventilation, and Air Conditioning

PV Photovoltic

1. INTRODUCTION

Photovoltaic (PV) systems at residential and commercial properties are a common method for generating electricity near the point of consumption. The U.S. is experiencing substation growth in PV installations. According to [5], between 2009 and 2020 the residential installed capacity increased by about 44%. Over the same time period the total capacity of PV systems at commercial buildings went up by just over 18%. Utilities have little influence over roof-top distributed PV installations and most are likely installed based on customer motivations and available finances. This means that a majority of the installations do not follow a prescribed planning approach as suggested in past work [6].

An accurate representation of PV adoptions entails the consideration of spatial variation. This work assumes that across a single city the solar availability is equal on average. And, PV system installation locations within a single city depend on the spatial disparity associated with income and building types. The examination considers installation trends within different median income census and building zoning areas to predict new adoptions throughout a city.

After completing the PV adoption forecast, this work then executes an impact study that defines the potential change in performance associated with the increase in distributed PV in future years. The approach considers both distribution and sub-transmission grid operations throughout an entire city. In this case, the city of Santa Fe, New Mexico is studied via a synthetic model representation. The simulation effort includes existing and future PV integration levels that match with carbon emission reduction goal timelines (i.e. 2030, 2040, and 2050). The approach uses the integration levels at the different years to simulate the entire city's grid operations over time. This includes variable irradiance and power consumption profiles for different load types.

This large-scale simulation effort is important for understanding Electrical Power System (EPS) operations to help coordinate the transition from fossil fuel based electrical power generation to renewable energy. Mandates, such as the "Energy Transition Act" in New Mexico (NM) [8], require the elimination of carbon emissions in the electrical power sector, which implies a significant increase in renewable energy. The transition requires multiple new power generation sources to make up for the decommissioning of a fossil fuel dependent systems, such as the coal power plant in New Mexico.

Distributed PV systems can also play a role in system wide resilience by contributing to the operations of neighborhood scale microgrids. Potentially, the natural integration of PV can form resilience zones where the net energy is close or equal to zero for one to three days. This work examines this hypothesis by implementing a graph theory community detection algorithm to identify electrical communities. Using the modularity algorithm densely connected loads are grouped together and separate from sparse connections with other communities.

2. PRIOR WORK

A detailed understanding of existing and future generation and consumption will improve EPS planning. Planning assessments include hosting capacity studies for new Distributed Generation

(DG) [14] or Electric Vehicles (EV) [17, 18]. The research studies include sing-point simulations to understand location impacts [10] that define the potential infrastructure upgrades required to support the new PV system [38]. Typically, this iterative process loops through various PV sizes until a violation occurs and then moves to a new bus where the process repeats [32]. Other approaches consider the stochastic integration of PV [37] on distribution EPSs. Using the stochastic and single-point approaches, the Electric Power Research Institute (EPRI) created a hybrid tool to assess distribution system abilities to host both centralized and distributed PV [35]. Assessing the stochastic integration of PV also provides a means to evaluate the control requirements and risks associated with roof-top PV systems [16].

PV forecasts that predict future generation are useful for operations of the grid. This includes long-term next day PV generation predictions [23, 28] or short-term forecasts that use satellite or ground-based images to predict PV generation [11, 24]. Yet, little is known about long-term predictions that forecast how much and where distributed PV generation will be in 5, 10, 20, or 30 years into the future. An estimate of future integration levels is useful for grid infrastructure, generation, and grid controls planning.

This approach offers a unique perspective for understanding DG integration levels now and in the future. Unlike existing market research studies that examine the world [1] and country [31, 33] general trends, this approach provides specific insight for a particular transmission system region and multiple distribution systems. Similar work forecast residential solar deployment in California using a time-series forecast model, threshold heterogeneity diffusion model, a Bass diffusion model, and National Renewable Energy Laboratory's dSolar model [12]. Other work identified roof-top solar installation "hotspots" using financial and technical indicators and used the entire country of Thailand [40]. Also, an empirical analysis of counties in California identified the impact of economics on PV adoptions [20].

A full scale assessment of a city's electrical system has been performed in the past. For example, stochastic simulations of the grid were performed to assess demand response at a city-wide scale [27]. Existing literature also documents different hosting capacity studies that consider the impact of new systems like DG [14] or EV on various EPSs. The research studies include single-point simulations to understand location impacts [10] that define the potential infrastructure upgrades required to support the new PV system [38].

3. CITY-WIDE GRID MODEL

A wide-spread assessment of PV integration for performance and resilience across a significant area involves the modeling of an EPS that represents both sub-transmission and distribution. Unfortunately, large-scale models that represent actual systems are not available in the public domain. However, recent work in the area has resulted in the creation of synthetic EPS models [21, 26]. And, this work leverages a model that represents the EPS that serves residents in Santa Fe, New Mexico [19]. The development of the realistic representation of the EPS in Santa Fe, shown in Figure 3-1, considered building footprints, streets, and real grid data. The OpenDSS simulation software [3] version is available for public download [13].

The geographic representation of the City of Santa Fe EPS, shown in Figure 3-1, depicts transmission, sub-transmission, and distribution lines. Two transmission lines start at a fictional point in the north (top of the figure) and connect to two transmission substations inside the city. The sub-transmission system runs throughout the city and connects the transmission substations to 8 distribution system substations.

This EPS includes medium and low voltage lines that support over 84,000 customers. The lines extend over 1,921 km through 2 transmission substations, 8 sub-transmission substations and finally to 28 feeders. By default, these feeders provide over 194 MW to approximately 38,590 buildings located throughout the foothills and in more densely populated areas within the city.

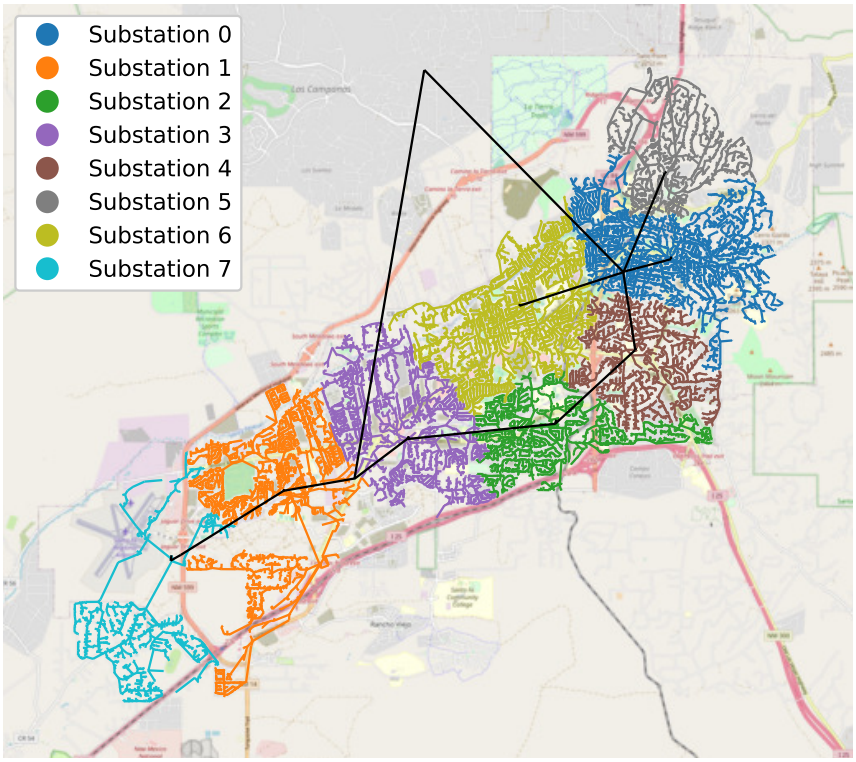

Figure 3-1 This map shows the electrical lines of the synthetic model that provide a realistic geographic representation for Santa Fe, New Mexico. There are two transmission lines from a fictional point in the north that connect to two transmission substations. The sub-transmission lines run throughout the city and connect the distribution substations.

4. PHOTOVOLTAIC SYSTEM INTEGRATION FORECAST

To gain a realistic understanding of current and future PV installations over a particular region, a review of installation locations and potential impact factors (e.g. income, building types) is necessary. This review involves an assessment process described in Figure 4-1.

The process begins with a review of spatial data, such as zoning, census, and historical PV installation patterns for the area of interest. Existing PV system locations are available through city and county public permit records. Municipalities may provide their permit data through web-based interfaces or the data is accessible through a public records request. Unfortunately, the public records may not provide the PV system capacity. The records typically describe a minimum amount of information such as the installation date and the physical address of the PV system.

This permit data can then be coupled with information on particular geographic areas that describe income levels and building types. For this analysis, the income levels come from readily available U.S. census data [7] and the building types are provided by city and county zoning area maps. For example, Santa Fe, New Mexico provides information through their GIS website [4].

This work implemented multiple steps, depicted in the Figure 4-1 flow diagram, to predict future PV. Prepossessing of the spatial and time dependent data beginning with combining the zoning and median income areas. This was achieved by performing a union that creates new districts. The union of the two spatial data sets identifies where they overlap geographically to create areas that represent both building type and income. Then, the historical PV permit data were mapped to the new income/building type districts. For each district, a least-squares regression model represents the linear change in PV installations that occurred over the last 11 years. As a result, each of the new districts have a linear model that predicts future growth in years: 2025, 2030, 2040, and 2050 for different income and building type districts. To test this methodology, this paper examines the spatial integration of PV over time in Santa Fe, New Mexico.

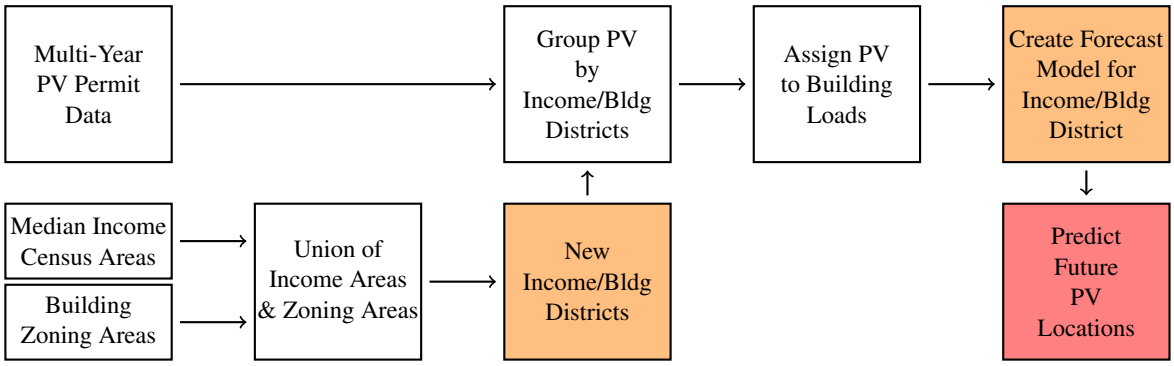

Figure 4-1 This flow diagram describes the assessment methodology used to predict future distributed PV locations. It begins with the assembly of PV permit data, median income census area data, and building zoning data. Then, a union of these geographic areas was performed to create new income/building districts. After that the PV permit data was grouped into each of the new districts and assigned to nearby building loads. The final step was to create a forecast model that provides predictions many years into the future.

4.1. Census & Zoning Geographic Regions

Two main factors for PV integration were considered. First, the median income of census block areas. Second, the type of building usage based on zoning designations defined by the local city and county codes.

Figure 4-2a depicts the median income census areas within four ranges. Areas where the median income was found to be below $40,000, between $40,000 and $60,000, from $60,000 and $80,000, and above $80,000. A majority of the city had median incomes between $60,000 and $80,000. The high incomes areas, where median income was above $80,000 tended to be in the outskirts of town.

The zoning districts, depicted in Figure 4-2b, included 10 different types such as parks (i.e. public), medical, commercial, and residential. Most of the city was found to be single-family and include densely populated areas with relatively small lots and larger lots in the mountain foothills. The downtown area, surrounding the plaza, was designated as business. Just outside this business area was multi-family structures. The commercial areas followed major driving areas, such as the busy Cerrillos Road in the middle of town. The industrial areas were in the southwestern part of the city near the local airport.

To assess the spatial and temporal aspects of PV installations, this work combined the median income and zoning areas into one mapping system. This was achieved by performing a union overlay of the income and zoning areas that preserved the unique regions and combined overlapping areas. Ultimately, this approach allowed for areas to have both income census and zoning labels. For instance, the single-family area in the eastern region of the city overlapped with the median income over $80,000 and became a single-family/$80,000 zone. The future PV integration predictions were then performed for each of the new union zones as described in the Section 4.3.

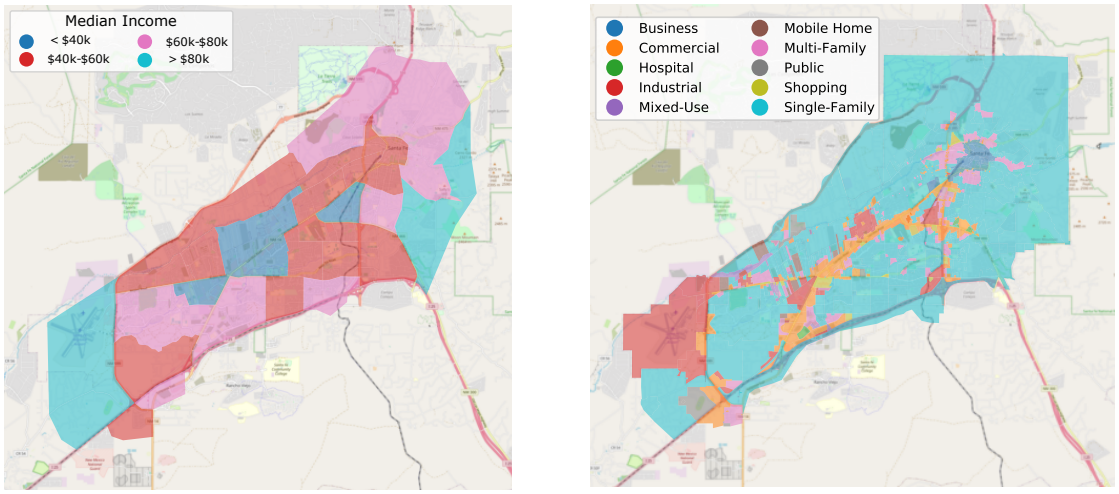

(a) Median Income Census Areas **(b) Zoning Districts**

Figure 4-2 The census median income areas is depicted in (a) and building zoning areas are shown in (b). These plots characterize the City's different neighborhoods by income and building use.

4.2. Historical Photovoltaic System Installations

An accurate representation of the existing PV integration involved the acquisition and review of PV construction permit records (depicted in Figure 4-3). According to the City of Santa Fe records about 1867 PV systems were installed since 2009. A query of the Santa Fe County permit database revealed that 5892 systems since 2009 were installed. Each of the over 7759 PV system locations were then mapped to geographic locations based on the provided street addresses.

This assessment focused on PV systems installed within the limits of a synthetic EPS model of the City of Santa Fe [13]. Some of the EPS electrical lines extended into areas under Santa Fe County jurisdiction. The mapping found that 1987 PV systems fell within the EPS model boundary as depicted in Figure 4-3. Figure 4-3 shows the boundary of the EPS and PV system locations colored based on the year of installation.

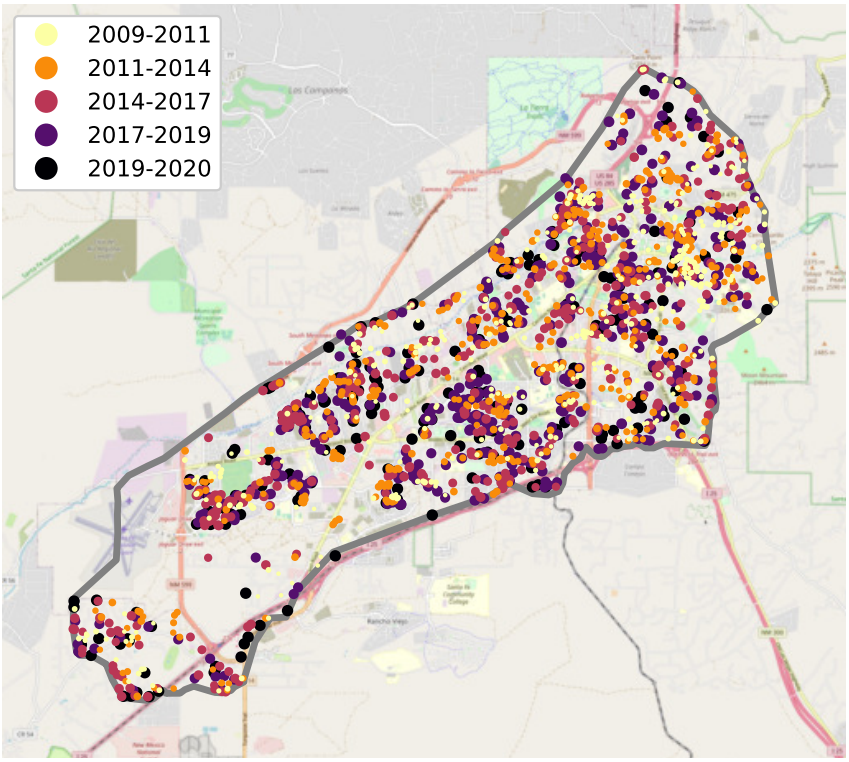

Figure 4-3 This map shows the photovoltaic system permit locations from 2009 to 2020 within the limits of the EPS model.

The adoption of PV across the City of Santa Fe varied depending on the zoning and income levels as shown in Figure 4-4. Figure 4-4 plots the number of PV systems and the percentage of loads with PV between 2009 and 2020. The dots in the three-dimensional plot are colored based on the zoning designations and their sizes depend on the areas median income level. Single- and multi-family residences had PV numbers well above the non-residential buildings. Commercial areas had comparable percentages of loads with PV but not nearly as many loads, and hence a lower number of total PV systems.

Figure 4-4 shows that both zoning and income levels play a role in PV adoptions. The different zoning areas, depicted by the different colors in Figure 4-4, experienced various PV installation rates. Figure 4-4 describes the percentage of the loads with PV (z-axis) and the total number of PV (x-axis) at each year between 2009 and 2020 (y-axis).

PV system adoptions in areas with income levels above $80,000 extended to just under 10% of the available loads with only 220 total PV systems in 2020. In comparison, single-family areas in the median income range between $40,000 and $80,000 had a higher number of PV systems (1310) but lower adoption percentages (less than 7%) in 2020. Single-family areas where the median income was below $40,000 had a total of 146 PV systems installed over th 11 year period. In this area the overall adoption rate as a percentage of the load was less than 5%.

The non-residential buildings also experienced linear trends over time. Figure 4-4 shows the adoption of PV for shopping, public, mobile-home, mixed-use, industrial, hospital, commercial, and business districts. Commercial and business areas had the most amount of new PV over time in comparison to other non-residential areas. The number of PV installations at non-residential loads seemed to depend on income levels. For instances, PV installations at commercial and business buildings withing census areas where median income was low had less than 5% of their buildings with PV, while medium to high income areas had PV on more than 5% of the loads.

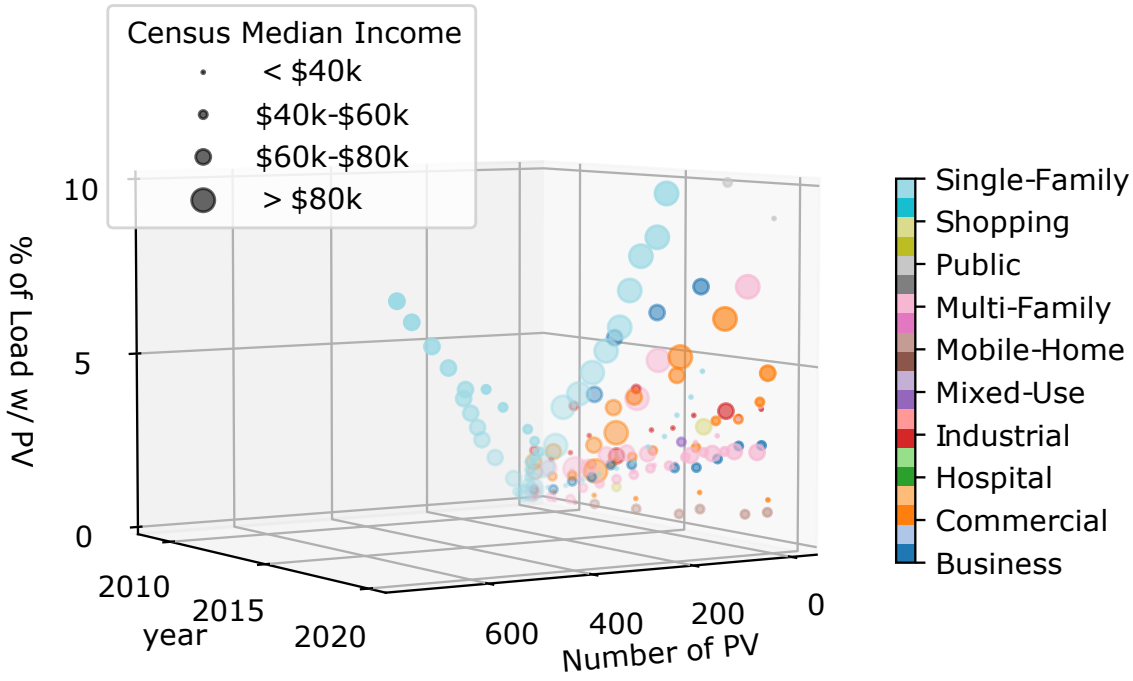

Figure 4-4 This figure depicts the increase in cumulative PV within the zoning and median income census areas. The plot describes the change in PV as a percentage of the number of loads (z-axis) and the total quantity of PV (x-axis).

4.3. Future Photovoltaic Integration Model

It was evident, from Figure 4-4, that the percentage of loads with PV tended to increase linearly between 2009 and 2020. If the trends persist, a data-driven linear function based on historical data will accurately estimate future PV installations.

Because of the linear behavior, this approach used a linear least-squares regression function to represent past installations and predict future numbers. A model representation for each of the new zones that represent income and building zoning areas (described in Section 4.1) allowed for both spatial and temporal forecasts to occur.

An optimization identified the free parameters (i.e. a and b in Equation 1) that produced the best fit for each new group's PV installation data.

$$y = ax^2 + b \tag{1}$$

The x, in Equation 1, represented time in years and y was the percentage of loads with PV for each new group. This output was then multiplied by the number of loads in each group to define the number of predicted PV installations at each future year. Then, the new PV systems were randomly assigned to loads without an existing PV system.

4.4. Mapping of Photovoltaic Systems to Model Loads

Existing and new PV systems were mapped to a load within the EPS model. The intent was to prepare the EPS model for simulations that include PV. The resulting model also supported a PV adoption analysis that evaluated future resilience by comparing PV generation with local energy demand to identify the gap between generation and consumption if it were to operate in microgrid mode.

The mapping of the PV to each load entailed the comparison of their latitude and longitude locations. This comparison involved the Python SciPy [39] KDTree nearest neighbor algorithm [25]. The assigning of PV to each load involved an iterative process. First, a list of available loads was generated. Then, each PV system's nearest neighbor was found using a distance of 0.01. Loads were not allowed to have more than one PV system, and all loads with PV were removed from the list of available loads. At this point the KDTree nearest neighbor compared the unassigned PV systems with the updated load availability list to find the next closest loads. This iterative process repeated until all of the PV systems within the city's boundary, depicted in Figure 4-3, were assigned to a load in the EPS model.

5. TRANSMISSION & DISTRIBUTION CO-SIMULATION

To support scalable simulation of a grid spanning a full city we developed a co-simulation environment that enables the use of separate simulators for each distribution system while still modeling the coupling between distribution systems through their connection to a common

sub-transmission circuit. The co-simulation environment is built on the HELICS library [30]. It consists of a single sub-transmission federate and one or more distribution system federates. The co-simulation environment separates the distribution and the sub-transmission systems at the bus where each sub-station is connected to the sub-transmission system. Each substation, including the transformer that steps down from sub-transmission to distribution voltage and the distribution feeders connected to it, is simulated in a single distribution system federate. The sub-transmission circuit, with all of its substations removed, is simulated in the sub-transmission federate.

At each simulation time step, the distribution system federates complete a power flow solution and then notify the sub-transmission system of the power demand on each phase at the point of common coupling (the high-voltage side of the substation transformer). When the sub-transmission federate is notified of a change in demand from a distribution system, the sub-transmission model is updated and a new power flow solution is evaluated. Based on the new solution, the voltage of each phase at each substation is updated and transmitted to the distribution system federate.

The co-simulation takes advantage of the co-iteration capability provided by HELICS which enables the exchange of boundary variables between federates multiple times at each simulation time step. This capability improves the fidelity of the simulation as it allows for tight coupling between simulators through convergence of variables that represent the physical state of the grid at the point of connection between the sub-transmission and the distribution systems without requiring the simulation time to advance. In the present work, convergence of the boundary variables is achieved through a fixed-point iteration on the power demand from each distribution system. Iteration proceeds until the change in the demand from all distribution systems is less than a fixed tolerance. Once the demand converged, the distribution federates are permitted to advance to the next time step. The operation of the distribution system and sub-transmission federates is described in detail in sections 5.1 and 5.2 respectively. Figure 5-1 provides an overview of the federates and the boundary variables that are exchanged between the federates.

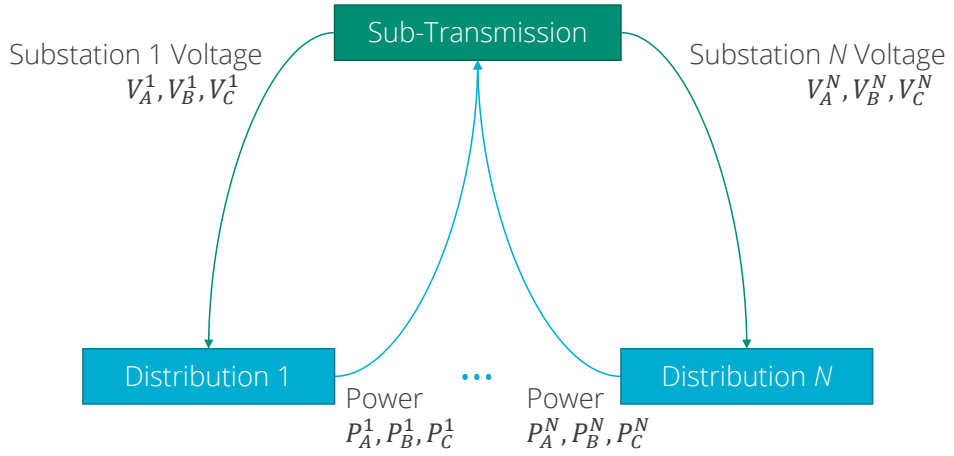

Figure 5-1 Co-Simulation overview. Boundary variables that are exchanged between simulators are shown. Power on each phase (P_A, P_B, P_C) is passed from each distribution system simulator to the sub-transmission simulator and the voltage on each phase (V_A, V_B, V_C) at the bus where the substation is connected is passed from the sub-transmission simulator to each distribution system simulator.

5.1. Distribution System Federate

The distribution system federate simulates the operation of an electric power distribution system using OpenDSS. The grid model simulated by the distribution system federate includes a single substation and all feeders that originate at that substation. As input, the distribution federate takes the voltage on each phase at the bus where its substation is connected to sub-transmission circuit. The simulation time is driven by events in the distribution system. Whenever a control action (e.g. a voltage regulator tap change) is scheduled to be executed, or at regular intervals (if there are no pending control actions), the distribution system federate evaluates a power flow solution and updates the boundary variables for the sub-transmission federate (power demand from the substation on each phase). If the demand at the substation has changed from the previous time, the sub-transmission simulation will be interrupted and a new iterative solution begins at the current time. In addition to solutions at the requested time, distribution system federates are preempted and evaluate a power flow solution whenever the substation voltage provided by the sub-transmission federate changes. The operation of the distribution system federate is shown in Figure 5-2.

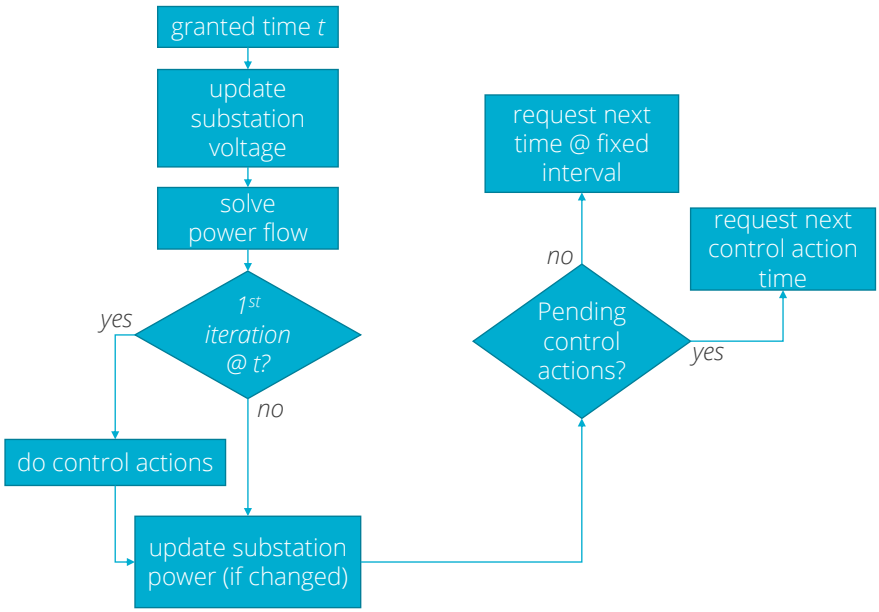

Figure 5-2 Operation of the distribution system federate. The distribution system federate is either granted its requested time or is preempted by a change in substation voltage provided by the sub-transmission federate.

Each distribution system records the total demand and PV generation, along with power quality data such as minimum and maximum voltage and thermal loading. To enable analysis of resource adequacy for microgrids based on existing PV generation, these statistics are recorded for arbitrary sections of the grid (for example, the communities identified by the methodology described in section 7) as well as the full distribution system model.

5.2. Sub-Transmission Federate

The sub-transmission federate simulates the operation of the sub-transmission circuit that distributes power from the transmission system to the distribution substations through out the city. Within the sub-transmission system model each distribution system is modeled as a set of three single-phase loads, each load representing the power demand on each phase from the substation. When the demand from one of the distribution systems changes, the sub-transmission federate evaluates a new power flow solution and updates the voltage for each distribution system federate. The operation of the sub-transmission system federate is shown in Figure 5-3.

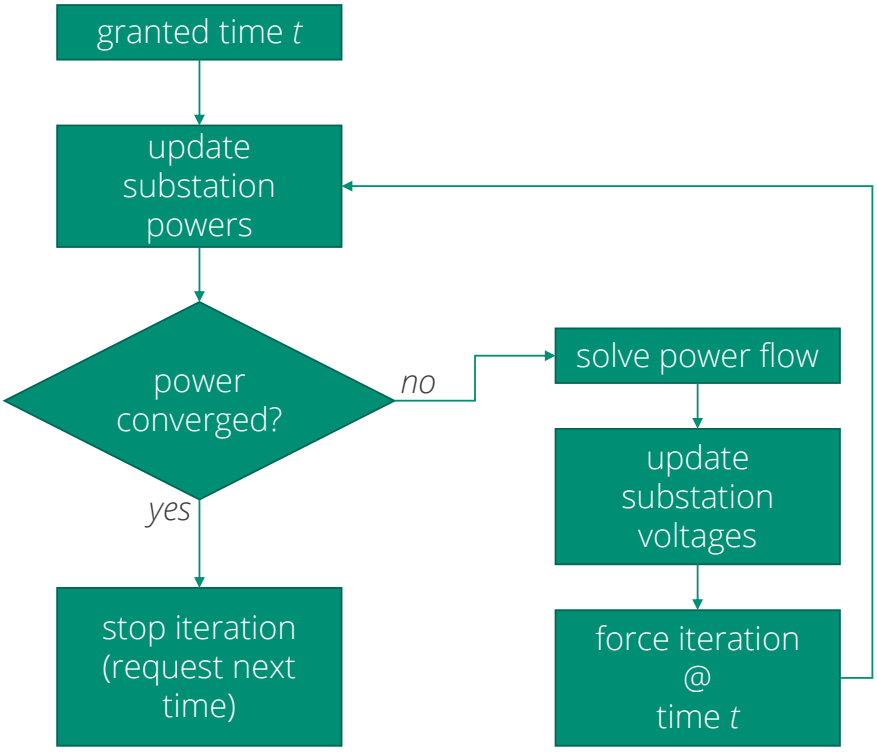

Figure 5-3 Operation of the sub-transmission federate. The sub-transmission federate is granted a new time whenever the demand from one of the distribution systems changes.

The sub-transmission system federate is responsible for managing convergence of the boundary variables at each time step. The solution is iterated at each time until the power demanded on each phase from each distribution system federate converges. For the present work we implemented a simple fixed-point iteration to move the federates towards convergence. Until the demand from each distribution system converges the sub-transmission system will update the voltage at each substation and force the distribution systems to solve another power flow at the current time. Once demand from all distribution federates has converged, the iteration is complete and the distribution system federates are allowed to advance to the next solution time. This method was successful in achieving convergence in very few iterations (typically only one iteration) for the system we analyzed in this report.

5.3. Co-Simulation Performance

Because the co-simulation requires iterations to achieve convergence of the boundary variables multiple power flow solutions must be evaluated at each simulation time. By comparison a single model of the grid for the full city requires only a single power flow solution at each simulation time, but at the cost of a substantially larger and more complex model. We compared the performance of the co-simulation to the single model approach to asses the impact of both the increased number of power flow solutions and the reduced problem size that each co-simulation federate needs to solve. The single model approach was evaluated using the same program as used by each distribution system federate, but simulated the full city of Santa Fe grid model including the sub-transmission and all distribution system federates. This allowed for a comparison of the same time trajectory and the same data collection as the co-simulation. The results in Figure 5-4 show that despite the added computation required for iteration on the boundary variables at each simulation time step, the co-simulation achieves slightly better performance than the single-model simulation.

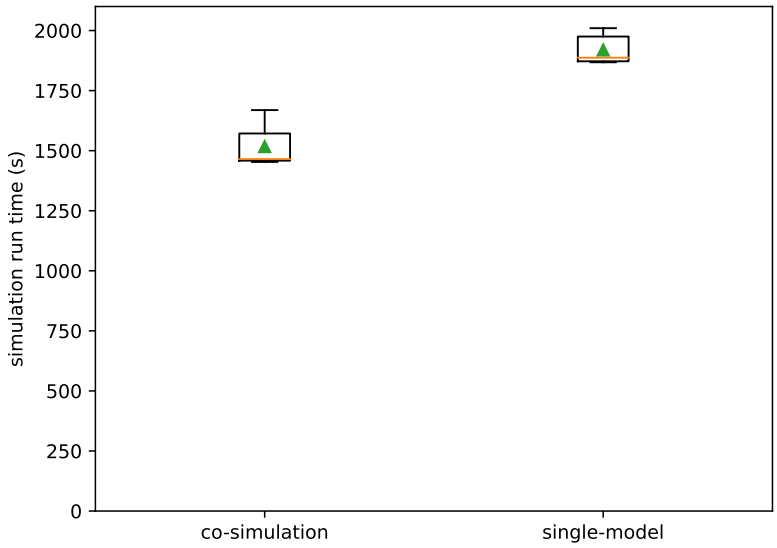

Figure 5-4 Comparison of wall time to run a week long simulation with the co-simulation and with a single simulator approach (single-model). Mean run time is marked by a green triangle.

6. CITY-WIDE TIME-SERIES SIMULATIONS

A city-wide PV hosting capacity evaluation defined the realistic impact of DG on both sub-transmission and distribution systems for current and future integration levels. The assessment effort began with the identification of PV system locations and sizes that resemble actual existing and future locations. Existing locations were provided by the city and county public permit record offices. The records describe the installation date and address of each PV

system within the city limits. This historical data and readily available census information provided inputs into a data-driven forecast algorithm that predicted future PV amounts and locations. These existing and future PV locations were then associated with loads in the PV model and included in the simulations that output line overloading, voltage, and frequency metrics throughout the entire system as PV increase over the next 20 to 30 years.

6.1. Simulation & Analysis Methodology

The EPS simulations evaluated the integration of realistic PV adoption levels dispersed throughout the city of Santa Fe. The simulation effort began by producing and assigning load profile data to different building types. The load profiles were mapped to loads in the EPS model based on the zoning area map. Also, irradiance profiles for an entire week were provided to the OpenDSS PV models. The PV and load data was used by the distribution model and run alongside the sub-transmission in the co-simulation environment.

The simulations assumed each of the PV systems were installed at a nearby load. The size of the PV was set to be 135% of the rated load defined by the OpenDSS model. The sizing of the PV followed the approach described in [16] where a PV capacity of 135% of the rated load resulted in a 100% offset of the annual energy consumption for typical residential and commercial buildings.

6.2. Load Demand Profiles and Photovoltaic Shape Descriptions

Data about Santa Fe was collected and applied to the synthetic system simulation for more realism. This data included: PV irradiances values, temperature, and load profiles.The data set used for PV and temperature data was obtained from the National Solar Radiation Database (NSRDB) which uses geostationary satellites to gather information for 4 km x 4 km gridded segments of the United States in half hour increments [29]. Figure 6-1 shows the synthetic system of Santa Fe with a transparent square indicating the location of data selected from the NSRDB.

To simulate a summer scenario, with high air-conditioning power demands, the week containing the highest temperature was identified and the associated data was collected. The values of interest to this project from NSRDB data were clear sky global horizontal irradiance (GHI), actual GHI, and temperature. GHI can be thought of as useful irradiance present at a PV module while clear sky GHI data ignores any reduction in irradiance due to cloud cover. To use the NSRDB data in the OpenDSS synthetic model, GHI values were normalized to $1000\ W/m^2 = 1\ PU$. Figure 6-2 depicts the week of temperature and GHI data that was selected.

Load profiles for buildings were collected from a Typical Meteorological Year 3 (TMY3) data set released by NREL in 2014 [41]. Electric power usage information corresponding to Santa Fe buildings were selected from the same week that contained the highest temperature in the NSRDB data and then normalized to the week's maximum to be applied as a scaling factor to the default model load values. Half hour load data was generated from the hourly data using a quadratic interpolation method available in the Pandas Python package.

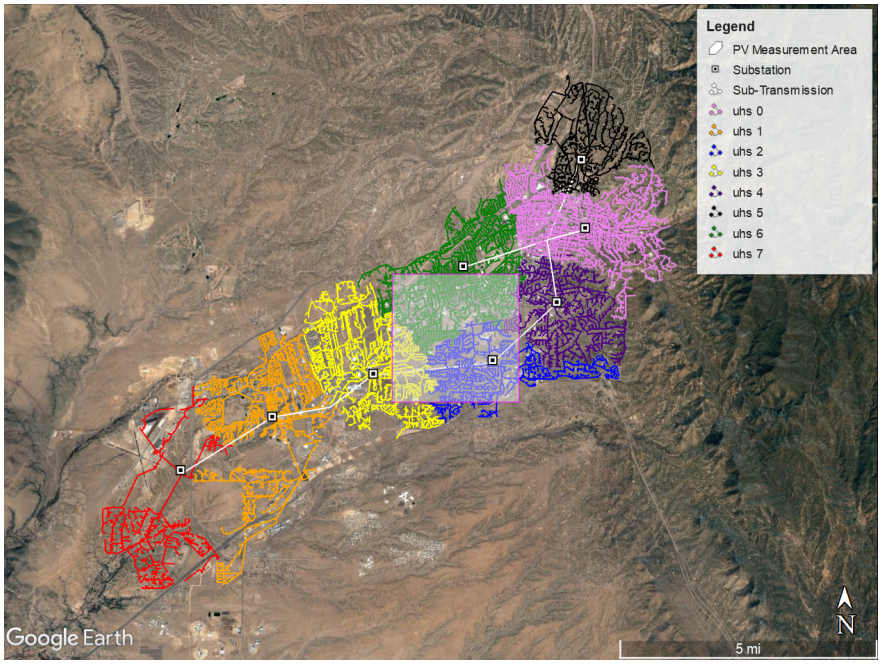

Figure 6-1 Synthetic System of Santa Fe with NSRDB Data Location Overlay.

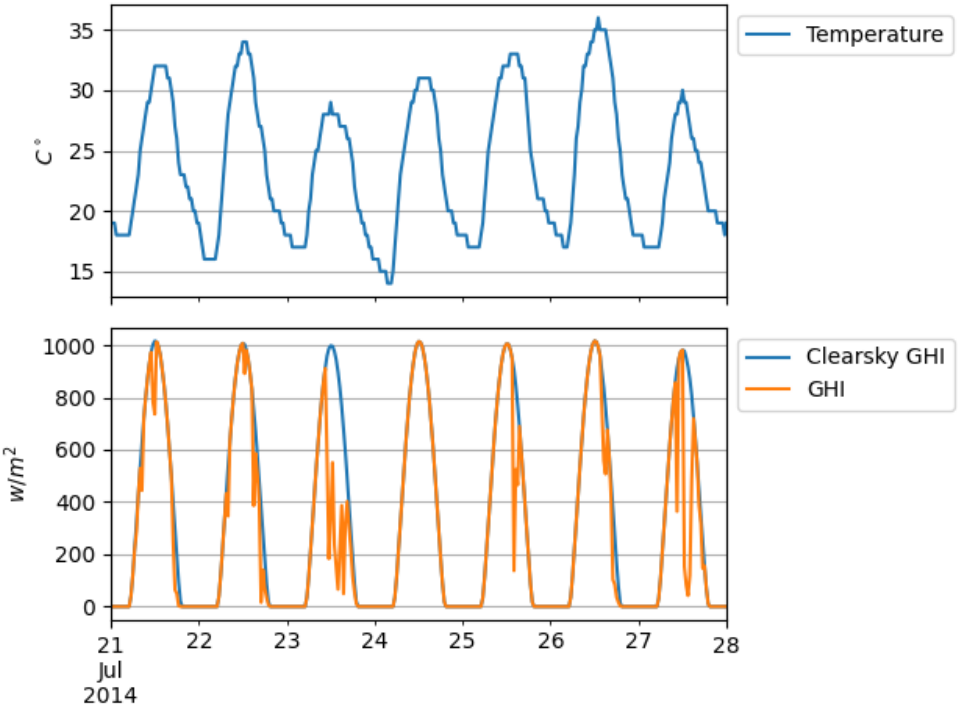

Figure 6-2 Collected Temperature and GHI Data.

As the TMY3 data set contains different profiles for specific types of buildings, a 'zone to building' mapping was created based on available zoning information. This mapping is presented as Table 6-1 while the resulting PU load shapes are shown in Figure 6-3. It should be noted that

due to excessive system overloading issues, the load shapes were scaled by 75% for simulations are also shown in Figure 6-3.

Table 6-1 Zoning to Load Shape Mapping.

Load in Zoning District	Applied TMY3 Data Set
Single-Family	Residential Base
Multi-Family	Mid-Rise Apartment
Shopping	Strip Mall
Business	Medium Office
Industrial	Warehouse
Commercial	Super Market
Hospital	Hospital
Mobile Home	Residential Low
Mixed-Use	Quick Service Restaurant
Public	Super Market

Figure 6-4 shows the total number of loads mapped to each category and the associated load values at 1 PU for the entire synthetic Santa Fe model. It can be seen that most loads and power consumption was classified as Single Family. While this mapping may be realistic, the Single Family shape contains a very large evening spike which may not be particularly realistic. Figure 6-5 shows that The residential load shapes from the TMY3 data report heating, ventilation, and

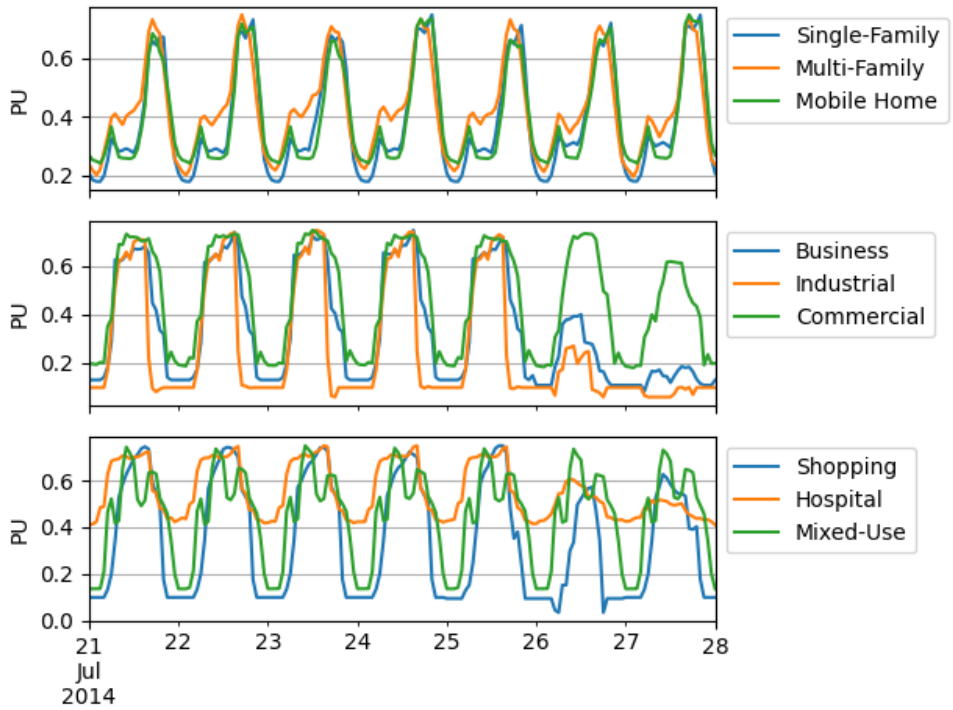

Figure 6-3 PU Load Shapes Created from TMY3 Data.

air-conditioning (HVAC) make up about 30%-40% of the evening demand.

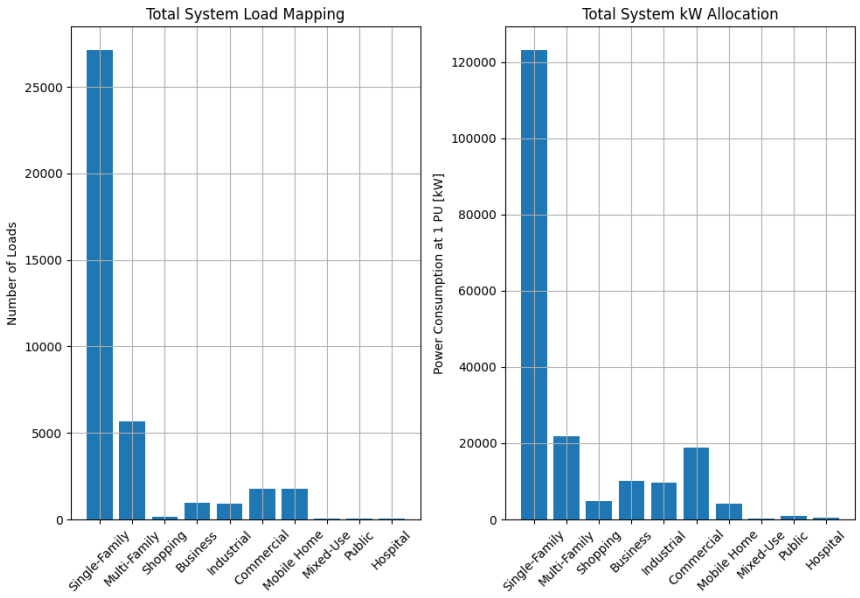

Figure 6-4 Total System Load Shape Mapping Information at 1 PU.

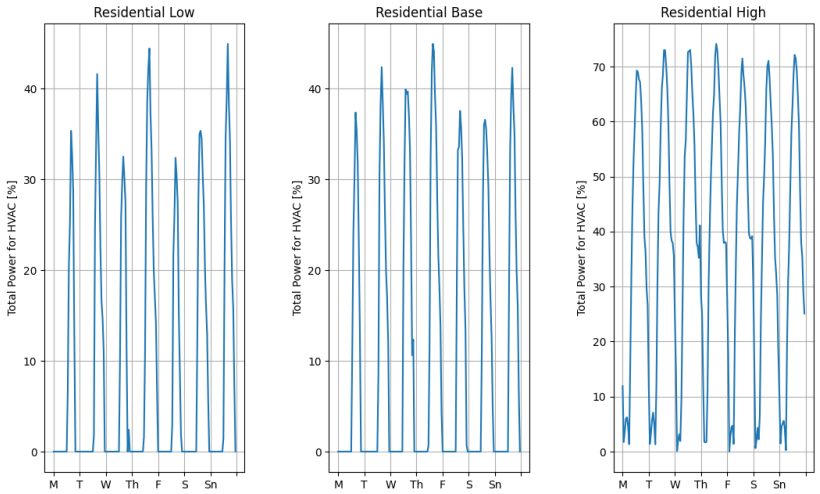

Figure 6-5 Residential Load Shape HVAC Percentage.

7. NEIGHBORHOOD MICROGRID IDENTIFICATION

7.1. Graph Theory Community Detection

This work used the modularity maximization method to define the potential microgrid zones inside the city's EPS. The method can divide the grid into multiple even groups [22]. An even

distribution of the nodes and an optimal number of groups results in a configuration where microgrids scattered throughout the city can be managed efficiently.

A form of the modularity maximization, known as the Clauset-Newman-Moore greedy modularity maximization [9], divided the distribution lines into sections that can potentially be organized during a grid outage into a functioning microgrid that supports individual neighborhoods. To do this, the algorithm cycled through multiple iterations to find divisions that produce the highest modularity. The method calculated the fraction of edges that join vertices into a community using Equation 2:

$$e_{ij} = \frac{1}{2m} \sum A_{vw} \delta(c_v, i) \delta(c_w, j) \tag{2}$$

where m represents the number of edges in the graph, A_{vw} was the adjacency matrix of the network that was 1 if vertices v and w were connected and zero otherwise, c represents the communities, δ was 1 if the community was equal to the edge and 0 otherwise. The fraction of the ends of the edges was defined by:

$$a_i = \frac{1}{2m} \sum k_v \delta(c_v, i) \tag{3}$$

where k_v was the sum of A_{vw}.

Then, the modularity represented by Q, was defined by the top part of Equation 4 and simplified to be the sum of the edges minus the square of the fraction of edge ends attached to the vertices in a given community, i.

$$\begin{aligned} Q &= \frac{1}{2m} \sum \left[A_{vw} - \frac{k_v k_w}{2m} \right] \sum \delta(c_v, i) \delta(c_w, j) \\ &= \sum (e_{ii} - a_i^2) \end{aligned} \tag{4}$$

7.2. Contribution of Distributed Photovoltaic Systems in Neighborhood Microgrid

After adding PV to the EPS and defining neighborhood microgrid boundaries, the next step in the analysis was to define the contribution of PV for a single day of off-grid operations. The contribution was defined by comparing the total demand and generation energy for one day within each potential microgrid. Since the new microgrid communities were formed without consideration of PV generation or load consumption, the approach will likely result in microgrid communities where the PV does not offset a significant amount of the demand.

8. RESULTS

8.1. Union of Income and Zoning Areas

Combining the census and zoning polygons using a union overlay produced 31 new groups, depicted in Figure 8-1. These new groups captured both income and building type information. It

was achieved by performing a union overlay, which preserved the unique regions and combined overlapping areas. For instance, the single-family area in the eastern region of the city overlapped with the median income census areas over $80,000 and become a single-family/$80,000 group.

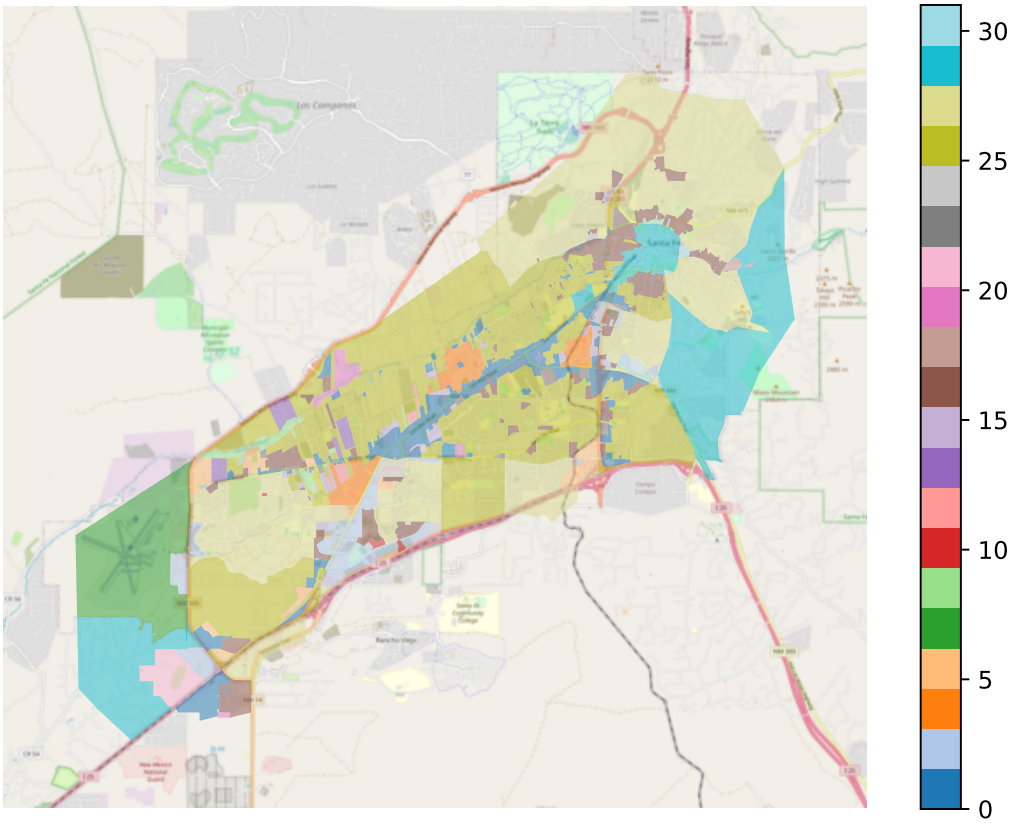

Figure 8-1 The union of the census and zoning data resulted in 31 new groups that captured both income and building use types.

8.2. Photovoltaic System Integration Forecasts

A prediction of future PV integration levels was performed for the different economic and build type areas described by the union of the median income and zoning regions in Figure 8-1. The number of PV systems from 2009 to 2020 in each of these regions is depicted in Figure 4-4. The three dimensional plot shows how the number of PV systems and the percentage of loads with PV change over the 10+ year period. This data was used to create the 31 different linear models to estimate future PV installations. The past and future installations for the entire region and specific areas are shown in Figure 8-2.

The overall city trend between 2009 and 2020 showed that the total percentages of loads with PV rose from 0.27% to 5.24% throughout the city. This progression exhibited a linear behavior, with a slight drop in installations in 2016, as shown in Figure 8-2. In 2010, none of the regions throughout the city had a percentage of their loads with PV above 4%. This changed over the ten

year period. For example, high income residential areas experienced an increase that resulted in 13% of the loads with PV. At the same time medium income residential areas went up to 8% of the loads with PV.

It was clear that during the observed time period in Santa Fe the percentage of loads with PV increased more dramatically for residential areas and not as much in commercial zoning districts. From 2009 to 2020 the number of PV systems increased from 9 to 160 for multi-family which equated to a percentage change of 0.18% to 2.85%. Single-family dwellings went from 77 (0.28% of loads with PV) in 2009 to 1675 (6.2% of loads with PV) in 2020. The downtown area of Santa Fe was designated as business and had 24 PV systems or about 6% of the loads had PV as of 2020. The commercial areas recorded 50 PV systems installed between 2009 and 2020 which was estimated to be about 4.5% of the loads in that type of zoning.

Using the linear model created based on data from 2009 to 2020 PV adoptions were predicted to reach 17.8% of loads in 2050 as shown in Figure 8-2. In the next five years (i.e. 2025) the number of loads with PV will likely reach 7.2%. The 2030 projection estimates that just over 9% of the loads will have PV. By this time higher income areas will have between 19-25% of their loads with PV and the medium income residential will be between 13 and 19%. The downtown business area will also experience an increase in solar installations and have between 8-13% of the loads with PV.

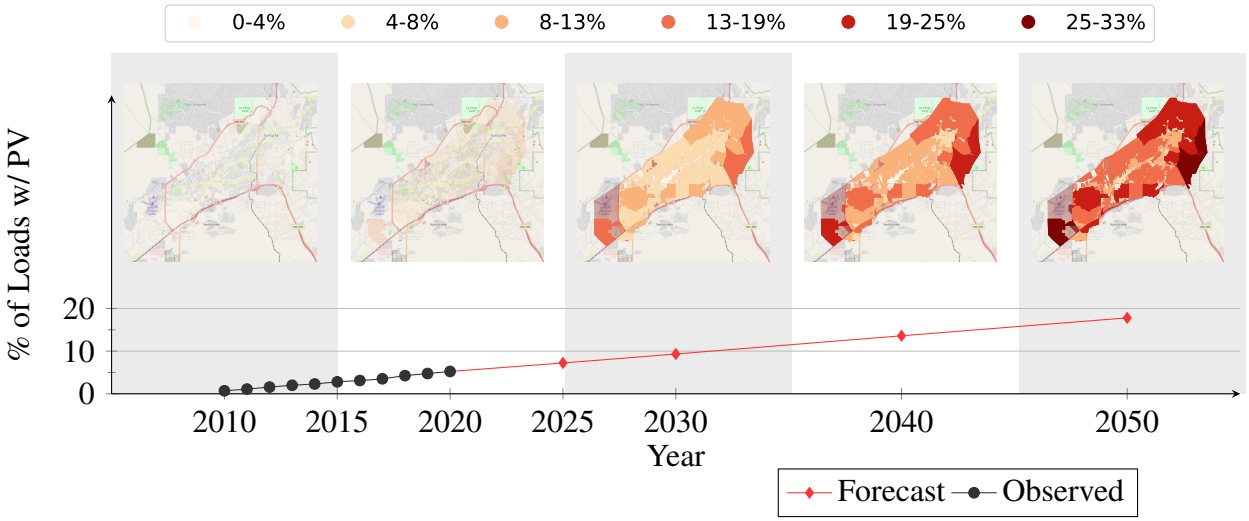

Figure 8-2 This plot depicts the change in the percentage of loads with PV from 2010 to 2050. Between 2010 and 2020 the data was extracted from actual permit records and the red line between 2020 and 2050 represents the model's prediction. The top part of the figure describes the spatial change in the percentage of loads with PV. The most drastic change in high income residential areas and the least amount of change was observed in industrial and mixed use zoning districts.

8.3. City-Wide Simulations

The co-simulation generated performance metrics for the distribution and sub-transmission systems. The results include generation, load, and voltage throughout the city at 2020, 2030, 2040, and 2050 PV adoption levels.

8.3.1. Distribution Systems

The simulation emulated operations over a seven day period and Figure 8-3 describes results for a single day when the PV generation caused the net load to reach its lowest value. The column on the left side of Figure 8-3 shows the net power and mean voltage across all of the distribution systems. At 2020, 2030, and 2040 levels the net power during the middle of the day when PV generation was at its peak (indicated by the circle, star, triangle, and square markers in Figure 8-3 time-series plots) did not fall below the early morning power demand. The 2050 PV generation resulted in a net power slightly below the night time demand.

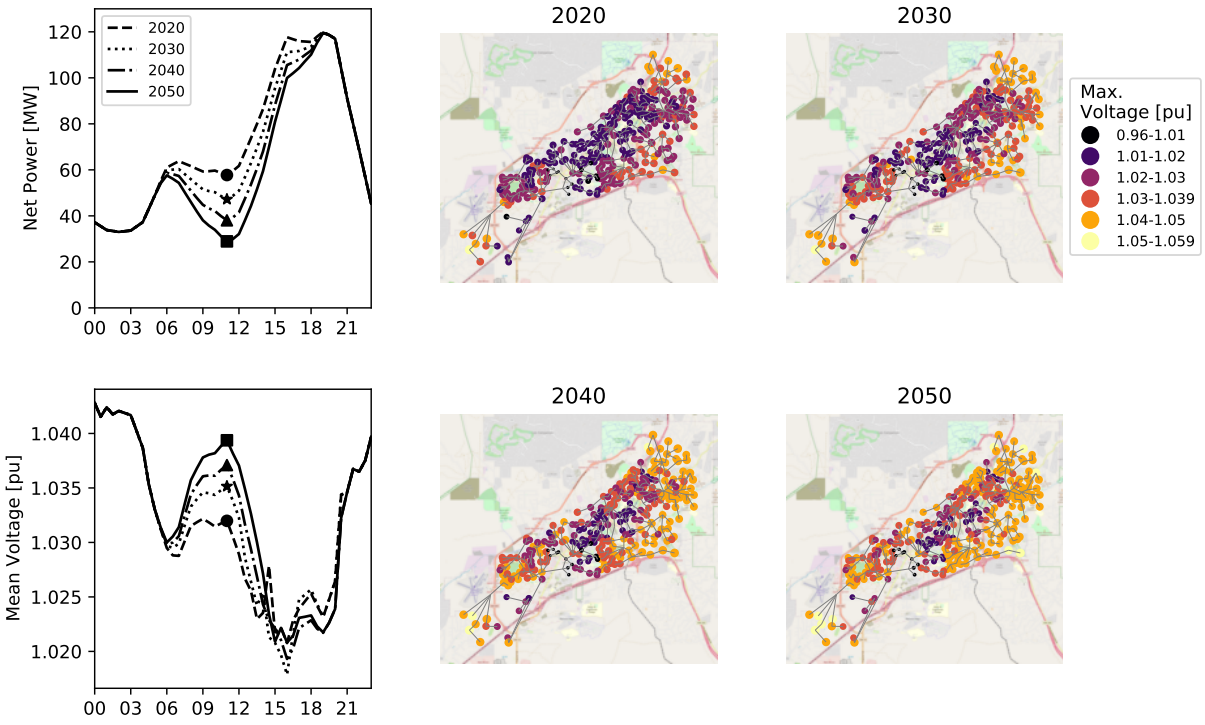

Figure 8-3 The simulation results showed that the distributed PV adoptions in 2020, 2030, 2040, and 2050 caused the net power to decrease by significant amounts. The change in net power resulted in average voltages reaching close to 1.04 pu and the maximum voltages in some areas of the city exceeded 1.05 pu.

Daytime PV generation scattered throughout the city caused the voltage to increase from about 1.032 p.u to 1.039 p.u between 2020 and 2050 levels as depicted in the bottom plot in the left column of Figure 8-3. The new PV adoptions did cause voltages to vary spatially, as shown in the images on the right side of Figure 8-3. For instance, the 2020 adoption levels produces simulation results where many of the the highest voltages were observed in the north east section of the city where PV adoptions were highest. As PV increased to 2030, 2040 and 2050 adoptions levels, the voltage increased overall throughout the city, but especially in areas where PV was installed the most (i.e high income single-family districts). In areas with high PV adoptions in 2050 the maximum voltage exceeded 1.05 p.u.

8.3.2. Sub-Transmission System

Figure 8-4 shows sub-transmission total power demand, overall PV power generation, and the maximum voltage at 2020, 2030, 2040, and 2050 adoptions. The simulation utilized the GHI PV shape which included variable generation on most days and one clear sky day. Under clear sky conditions, the peak PV power generation exceeded 40 MW, which in some instances was about half of the power demand. When the PV generation ramps down at the end of each day, the system net power ramp increased with higher PV penetration.

The distributed PV generation had little affect on maximum voltages as shown in the bottom plot in Figure 8-4. The sub-transmission was able to maintain a voltage between 0.99 and 1.005 pu during the entire simulation and for each of the PV adoption scenarios, however, voltage regulators included in the distribution systems likely allowed for a smoothing effect.

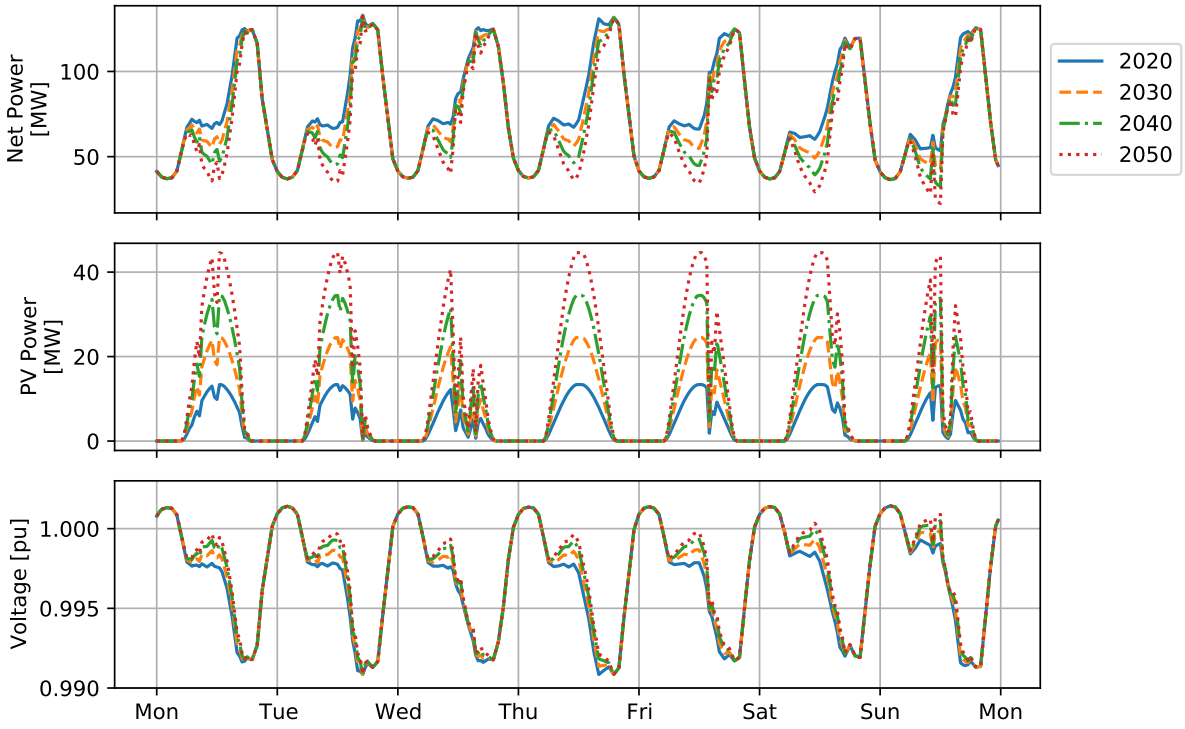

Figure 8-4 This figure plots the net power, PV power, and maximum voltage measured on the sub-transmission system. During the day, the PV power made a significant portion of the demand. Because of this, the voltage had a noticeable change for the different adoption rates. However, the change in maximum voltage was not significant enough to create an issues.

8.4. Distributed Photovoltaic Systems' Potential Microgrid Contribution

A review of distributed PV (at different adoption levels) contribution to potential microgrid operations involved a time-series simulation, the identification of communities, and an assessment of the consumption and generation energy for a single day. The simulation results, described in

Section 8.3, provided generation and demand at 30 minute intervals, which were used to compare the amount of generation needed to offset daily energy in each community.

8.4.1. Potential Microgrid Communities

Using the graph theory modularity algorithm 312 different communities were identified throughout the city. Each of the communities, that could act as a microgrid, are depicted with different colors in Figure 8-5a. A close up of a section of the city is shown in Figure 8-5b that shows the some of the communities and their interconnections. The work assumes that nearby or new switches could allow the sections to be segregated and operate as a microgrid on its own.

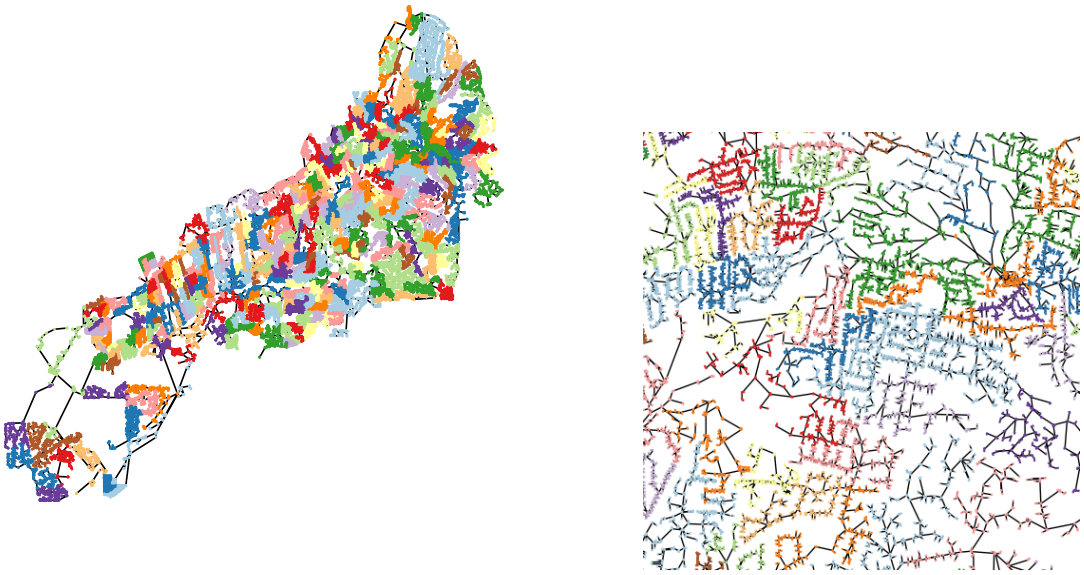

(a) Microgrid Communities **(b) Close Up of Communities**

Figure 8-5 (a) Depicts the 312 communities defined by the graph theory community detection algorithm. A close up view of the communities, in (b), shows the different groups and their interconnections.

8.4.2. Microgrid Communities Generation versus Consumption

The electrically connected communities may include distributed PV systems that can help offset the energy consumption while in microgrid mode. Figure 8-6 shows how the amount of PV generation over a single day compares to the energy consumption in the same community. The percentage of energy provided by the PV varies between 0 and 70.7% for 2020, 2030, 2040, and 2050 PV adoption scenarios.

The data shows that the increase in adoptions will improve the potential contribution of distributed PV in neighborhood microgrids. Under current 2020 adoption levels, the percentage of PV reached a high that was between 21.5% and 34.8% of the energy consumption in only five of the over 300 communities. This was projected to change with the increase in PV to 2030

adoption levels where 22 communities will have PV daily production that falls between 22% and 37% and 2 communities will have PV systems that offset consumption for 37% and 57% of the load's energy. In 2040, the change in PV results in 4 communities where just below half of the daily energy was offset by the PV. Finally, in 2050 five of the communities will have PV generation that will exceed 50% of the daily demand with one reaching as high as 70%.

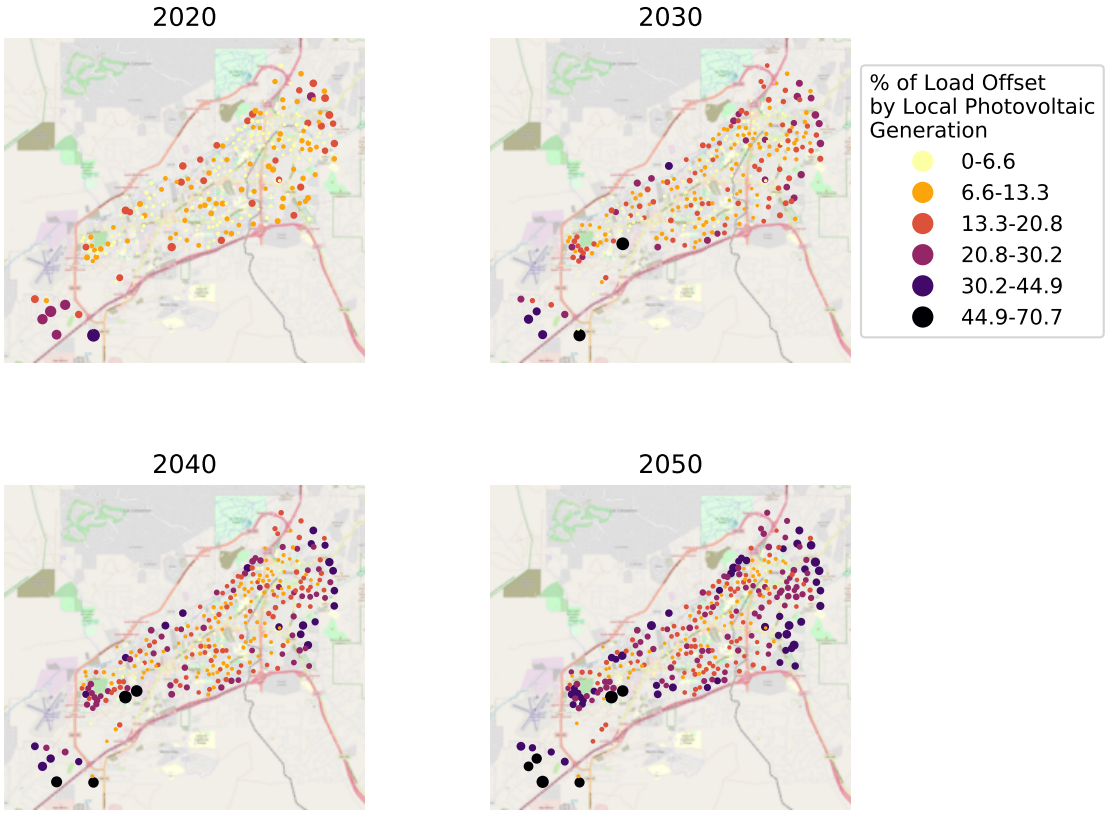

Figure 8-6 This figure depicts the percentage of each microgrid communities load will the distributed PV generation offset for 2020, 2030, 2040, and 2050 adoption levels. From 2020 to 2050 the percentage increases and results in many microgrid groups with PV percentages above 50%.

9. CONCLUSION

This report describes a simulation and analysis methodology that considers the integration of distributed PV throughout an entire city. The work began with the creation of a distributed, roof-top PV adoption forecast approach that predicts future installation locations in upcoming years 2030, 2040, and 2050 that considers spatial diversity (i.e. building types and income levels) and time-series historical trends (i.e. past PV installation permit records). Results form the PV adoption forecasts were then used as inputs into an EPS model that represented both distribution and sub-transmission. A week long simulation with the different PV adoptions that represent the various future years defined the impact on the EPS caused by roof-top PV sized to offset the local

loads annual energy. The simulations and a graph theory community detection algorithm reviewed the potential for PV to support (or contribute) to neighborhood microgrids scattered throughout the city's EPS.

Consideration of the spatial characteristics of the city led to a representative estimation of future PV locations. The approach combined the geographic income census and zoning maps to create 31 new groups. The PV trends from 2009 to 2020 indicated that the highest adoption rates occurred in residential areas with high income levels. These trends were carried through into future years which resulted in peak PV power outputs that went from 16 MW in 2020, 25 MW in 2030, 35 MW in 2040, and about 44 MW in 2050.

The addition of new PV generation scattered throughout the grid impact the overall net power. However, the impact on the sub-transmission voltage was very minimal. The distribution systems, on the other hand, experienced an increase that resulted in maximum voltages over 1.05 p.u for short periods of time. Also, the maximum voltage varied spatial across the EPS distribution systems and was the highest in areas where the PV adoptions were predicted to be the most significant.

Using the graph theory modularity community detection algorithm the EPS was broken out into 312 groups where the loads were densely situated. The grouping of the loads inside each group meant that they were ideally situated geographically to act as a microgrid during a grid outage. As PV adoptions increase, the potential impact on the neighborhood microgrids increases. In 2050, for example, the PV generation for a one day period will account for over 50% of the energy consumption. Future research is required to improve the community detection to increase the percentage of load offset by local PV generation. Graph theory approaches that consider directed graphs, power and generation quantities, and others may be potential alternatives that will result in improvements to the community detection for microgrid detection.

This work also created Python tools that help administer the HELICS co-simulation platform. The new capability offers researchers the opportunity to simulate large EPS at different frequencies to perform various studies. The ability to simulate sub-transmission and distribution provides a platform for understanding DER impacts over a large geographic area. It also can incorporate new control methodologies for development and testing purposes.

REFERENCES

[1] By 2023, the World Will Have 1 Trillion Watts of Installed Solar PV Capacity. Section: Solar.

[2] Santa Fe County : Growth Management / Land Use : Geographic Information Systems : GIS Disclaimer of Liability.

[3] EPRI | Smart Grid Resource Center > Simulation Tool – OpenDSS, August 2021.

[4] GIS | City of Santa Fe, New Mexico, 2021.

[5] U.S. Solar Market Insight. Technical report, Solar Energy Industries Association and Wood Mackenzie, August 2021.

[6] Mohammadhafez Bazrafshan, Likhitha Yalamanchili, Nikolaos Gatsis, and Juan Gomez. Stochastic Planning of Distributed PV Generation. *Energies*, 12(459), 2019.

[7] US Census Bureau. Census.gov, 2021. Section: Government.

[8] Jacob Candelaria, Nathan P. Small, Mimi Stewart, Patricia Roybal Caballero, and Brian Egolf. ENERGY TRANSITION ACT, 2019.

[9] Aaron Clauset, M.E.J. Newman, and Cristopher Moore. Finding community structure in very large networks. *Phys. Rev.*, 70(6), December 2004.

[10] K. Coogan, M. J. Reno, S. Grijalva, and R. J. Broderick. Locational dependence of PV hosting capacity correlated with feeder load. In *2014 IEEE PES T D Conference and Exposition*, pages 1–5, April 2014.

[11] Lasanthika H. Dissawa, Roshan I. Godaliyadda, Parakrama B. Ekanayake, Ashish P. Agalgaonkar, Duane Robinson, Janaka B. Ekanayake, and Sarath Perera. Sky Image-Based Localized, Short-Term Solar Irradiance Forecasting for Multiple PV Sites via Cloud Motion Tracking. *International Journal of Photoenergy*, 2021:e9973010, July 2021. Publisher: Hindawi.

[12] Changgui Dong, Benjamin Sigrin, and Gregory Brinkman. Forecasting residential solar photovoltaic deployment in California. *Technological Forecasting and Social Change*, 117:251–265, April 2017.

[13] Tarek Elgindy, Carlos Mateo Garcia, Pablo Duenas Martinez, Bryan Palmintier, Fernando Postigo Marcos, Tomas Gomez San Roman, Fernando de Cuadra García, Venkat Krishnan, and Nicolas Gensollen. Santa_fe_synthetic_network. June 2020. Accepted: 2020-07-01T19:12:43Z Publisher: NREL.

[14] Sherif M. Ismael, Shady H. E. Abdel Aleem, Almoataz Y. Abdelaziz, and Ahmed F. Zobaa. State-of-the-art of hosting capacity in modern power systems with distributed generation. *Renewable Energy*, 130:1002–1020, January 2019.

[15] C. Birk Jones, Matthew Lave, and Rachid Darbali-Zamora. Overall Capacity Assessment of Distribution Feeders with Different Electric Vehicle Adoptions. In *2020 IEEE Power Energy Society General Meeting (PESGM)*, pages 1–5, August 2020. ISSN: 1944-9933.

[16] C. Birk Jones, Matthew Lave, Matthew J. Reno, Rachid Darbali-Zamora, Adam Summers, and Shamina Hossain-McKenzie. Volt-Var Curve Reactive Power Control Requirements and Risks for Feeders with Distributed Roof-Top Photovoltaic Systems. *Energies*, 13(17):4303, January 2020. Number: 17 Publisher: Multidisciplinary Digital Publishing Institute.

[17] C. Birk Jones, Matthew Lave, William Vining, and Brooke Marshall Garcia. Uncontrolled Electric Vehicle Charging Impacts on Distribution Electric Power Systems with Primarily Residential, Commercial or Industrial Loads. *Energies*, 14(6):1688, January 2021. Number: 6 Publisher: Multidisciplinary Digital Publishing Institute.

[18] C Birk Jones, Matthew J. Lave, and R. Darbali-Zamora. Overall Capacity Assessment of Distribution Feeders with Different Electric Vehicle Adoptions. In *IEEE Power & Energy Society General Meeting*, August 2020.

[19] Venkat Krishnan, Bruce Bugbee, Tarek Elgindy, Carlos Mateo, Pablo Duenas, Fernando Postigo, Jean-Séebastien Lacroix, Tomás Gómez San Roman, and Bryan Palmintier. Validation of Synthetic U.S. Electric Power Distribution System Data Sets. *IEEE Transactions on Smart Grid*, 11(5):4477–4489, September 2020. Conference Name: IEEE Transactions on Smart Grid.

[20] Lado Kurdgelashvili, Cheng-Hao Shih, Fan Yang, and Mehul Garg. An empirical analysis of county-level residential PV adoption in California. *Technological Forecasting and Social Change*, 139:321–333, February 2019.

[21] Hanyue Li, Jessica L. Wert, Adam Barlow Birchfield, Thomas J. Overbye, Tomas Gomez San Roman, Carlos Mateo Domingo, Fernando Emilio Postigo Marcos, Pablo Duenas Martinez, Tarek Elgindy, and Bryan Palmintier. Building Highly Detailed Synthetic Electric Grid Data Sets for Combined Transmission and Distribution Systems. *IEEE Open Access Journal of Power and Energy*, 7:478–488, 2020. Conference Name: IEEE Open Access Journal of Power and Energy.

[22] Guoqiang Lin, Siyan Liu, Aihua Zhou, Jiangpeng Dai, Bo Chai, Bo Zhang, Hongbin Qiu, Kunlun Gao, Yan Song, and Rui Chen. Community detection in power grids based on Louvain heuristic algorithm. In *2017 IEEE Conference on Energy Internet and Energy System Integration (EI2)*, pages 1–4, November 2017.

[23] H.J. Lu and G.W. Chang. A Hybrid Approach for Day-Ahead Forecast of PV Power Generation. *IFAC-PapersOnLine*, 51(28), 2018.

[24] Andrea Mammoli, Guillermo Terren-Serrano, Anthony Menicucci, Thomas P. Caudell, and Manel Martínez-Ramón. An experimental method to merge far-field images from multiple longwave infrared sensors for short-term solar forecasting. *Solar Energy*, 187:254–260, July 2019.

[25] Songrit Maneewongvatana and David M. Mount. Analysis of approximate nearest neighbor searching with clustered point sets. *arXiv:cs/9901013*, January 1999. arXiv: cs/9901013.

[26] Carlos Mateo, Fernando Postigo, Fernando de Cuadra, Tomás Gómez San Roman, Tarek Elgindy, Pablo Dueñas, Bri-Mathias Hodge, Venkat Krishnan, and Bryan Palmintier. Building Large-Scale U.S. Synthetic Electric Distribution System Models. *IEEE Transactions on Smart Grid*, 11(6):5301–5313, November 2020. Conference Name: IEEE Transactions on Smart Grid.

[27] B. Morvaj, B. Jurisic, and N. Holjevac. Stochastic simulation of the smart grid and demand response implementations on a city-wide scale. In *2013 36th International Convention on Information and Communication Technology, Electronics and Microelectronics (MIPRO)*, pages 1241–1246, May 2013.

[28] Alfredo Nespoli, Emanuele Ogliari, Sonia Leva, Alessandro Massi Pavan, Adel Mellit, Vanni Lughi, and Alberto Dolara. Day-Ahead Photovoltaic Forecasting: A Comparison of the Most Effective Techniques. *Energies*, 12(9):1621, January 2019. Number: 9 Publisher: Multidisciplinary Digital Publishing Institute.

[29] NREL. National Solar Radiation Database, 2021.

[30] Bryan Palmintier, Dheepak Krishnamurthy, Philip Top, Steve Smith, Jeff Daily, and Jason Fuller. Design of the helics high-performance transmission-distribution-communication-market co-simulation framework. In *2017 Workshop on Modeling and Simulation of Cyber-Physical Energy Systems (MSCPES)*, pages 1–6, 2017.

[31] Julia Pyper. US Residential and Utility-Scale Solar Markets See Installations Fall for the First Time. Section: Solar.

[32] Matthew J. Reno, Kyle Coogan, John Seuss, and Robert Joseph Broderick. Novel Methods to Determine Feeder Locational PV Hosting Capacity and PV Impact Signatures. Technical Report SAND2017-4954, Sandia National Lab. (SNL-NM), Albuquerque, NM (United States), May 2017.

[33] Joshua Rhodes. The Future Of US Solar Is Bright, 2020. Section: Energy.

[34] M. Rylander, J. Smith, D. Lewis, and S. Steffel. Voltage impacts from distributed photovoltaics on two distribution feeders. In *2013 IEEE Power Energy Society General Meeting*, pages 1–5, July 2013.

[35] M. Rylander, J. Smith, and L. Rogers. Impact Factors, Methods, and Considerations for Calculating and Applying Hosting Capacity. Technical Report 3002011009, Electric Power Research Institute, Palo Alto, CA, February 2018.

[36] J. Smith. Stochastic Analysis to Determine Feeder Hosting Capacity for Distributed Solar PV. Technical Report 1026640, Electric Power Research Institute, Palo Alto, CA, December 2012.

[37] J. W. Smith, R. Dugan, M. Rylander, and T. Key. Advanced distribution planning tools for high penetration PV deployment. In *2012 IEEE Power and Energy Society General Meeting*, pages 1–7, July 2012.

[38] Sky Stanfield and Safdi Stephanie. Optimizing the Grid: Regulator's Guide to Hosting Capacity Analyses for Distributed Energy Resources. Technical report, Interstate Renewable Energy Council, December 2017.

[39] Pauli Virtanen, Ralf Gommers, Travis E. Oliphant, Matt Haberland, Tyler Reddy, David Cournapeau, Evgeni Burovski, Pearu Peterson, Warren Weckesser, Jonathan Bright, Stéfan J. van der Walt, Matthew Brett, Joshua Wilson, K. Jarrod Millman, Nikolay Mayorov, Andrew R. J. Nelson, Eric Jones, Robert Kern, Eric Larson, C. J. Carey, İlhan Polat, Yu Feng, Eric W. Moore, Jake VanderPlas, Denis Laxalde, Josef Perktold, Robert Cimrman, Ian Henriksen, E. A. Quintero, Charles R. Harris, Anne M. Archibald, Antônio H. Ribeiro, Fabian Pedregosa, and Paul van Mulbregt. SciPy 1.0: fundamental algorithms for scientific computing in Python. *Nature Methods*, 17(3):261–272, March 2020. Bandiera_abtest: a Cc_license_type: cc_by Cg_type: Nature Research Journals Number: 3 Primary_atype: Reviews Publisher: Nature Publishing Group Subject_term: Biophysical chemistry;Computational biology and bioinformatics;Technology Subject_term_id: biophysical-chemistry;computational-biology-and-bioinformatics;technology.

[40] Wichsinee Wibulpolprasert, Umnouy Ponsukcharoen, Siripha Junlakarn, and Sopitsuda Tongsopit. Preliminarily Screening Geographical Hotspots for New Rooftop PV Installation: A Case Study in Thailand. *Energies*, 14(11):3329, January 2021. Number: 11 Publisher: Multidisciplinary Digital Publishing Institute.

[41] Eric Wilson. Open Energy Data Initiative (OEDI), 2021.

DISTRIBUTION

Email—Internal

Name	Org.	Sandia Email Address
Charles Hanley	8810	cjhanley@sandia.gov
Summer Ferreira	8812	srferre@sandia.gov
Craig Lawton	8141	crlawto@sandia.gov
C. Birk Jones	8812	cbjones@sandia.gov
Technical Library	01977	sanddocs@sandia.gov

Sandia National Laboratories

Sandia National Laboratories is a multimission laboratory managed and operated by National Technology & Engineering Solutions of Sandia LLC, a wholly owned subsidiary of Honeywell International Inc., for the U.S. Department of Energy's National Nuclear Security Administration under contract DE-NA0003525.